IEEE Access
Multidisciplinary ⋮ Rapid Review ⋮ Open Access Journal

Received July 26, 2020, accepted August 2, 2020, date of publication August 5, 2020, date of current version August 17, 2020.

Digital Object Identifier 10.1109/ACCESS.2020.3014558

Optimization of the ISP Parameters of a Camera Through Differential Evolution

LUIS V. HEVIA[1], MIGUEL A. PATRICIO[2], (Member, IEEE), JOSÉ M. MOLINA[2], (Member, IEEE), AND ANTONIO BERLANGA[2], (Member, IEEE)

[1]BQ Engineering Team, 28232 Las Rozas-Madrid, Spain
[2]Applied Artificial Intelligence Group, Universidad Carlos III de Madrid, 28270 Colmenarejo, Spain

Corresponding author: Miguel A. Patricio (mpatrici@inf.uc3m.es)

This work was supported in part by the Private Research Project of the Company BQ, and in part by the Public Research Projects of the Spanish Ministry of Economy and Competitiveness (MINECO) under Grant TEC2017-88048-C2-2-R, Grant RTC-2016-5595-2, Grant RTC-2016-5191-8, and Grant RTC-2016-5059-8.

ABSTRACT Within the design and development of a smartphone, an important phase arises regarding time, which is related to the tuning of the ISP (image signal processor) of the camera. The ISP is an element that allows the adjustment of the images captured by a sensor in order to achieve the best image quality. The ISP implements different image improvement algorithms such as white balancing, denoising, and demosaicing as well as other image enhancement algorithms. The purpose of the ISP tuning process is to configure the parameters of these algorithms so that the processed images are of the highest quality. This task is carried out by the camera tuning engineer, who iteratively adjusts the ISP parameters through trial and error procedures until the desired quality is achieved. The complete adjustment process can be extended to several weeks and even months. The authors present a novel solution based on differential evolution, which allows a first-adjusted approximation of the ISP in a few hours. This work presents an architecture based on an optimization through a differential evolution algorithm with which different ISP tuning tests are carried out, and the good results in quality and time are verified.

INDEX TERMS Differential evolution, ISP tuning, smartphone design.

I. INTRODUCTION

Smartphones have become something beyond devices with a simple communication function. These devices are made up of a set of sensors that allow the creation of the most innovative applications [1]–[5]. Undisputedly, the most important sensor is the camera [6]–[9]. Mobile manufacturing companies always seek to improve the photographic quality of their cameras at all levels [10]. This rationale has been carried out to such an extent that now, the sights of many of these companies have been set on artificial intelligence to achieve this goal. This improvement can be achieved in different ways, for example, through photographic filters that are most sought after by users, such as portrait mode, where Google has stood out with its Pixel 2, which contains an excellent portrait mode owing to the help of neural networks [11].

Nevertheless, filters are not the only way to improve photographic quality; the other important part of image quality is its processing. For this task, there is a chip in the camera called the ISP (image signal processor) [12]. This chip performs the job of interpreting the photons that reach the sensor and processes the colors, but it can also perform other functions, such as noise reduction, edge enhancement, dynamic range processing and other types of adjustments and filters. This chip can greatly change the perception of an image without the user having to do anything, but its adjustment is a factory-based implementation or it is upgradable by the seller. It is key that this chip is well tuned so the camera can take good quality images from the start. However, since it is able to do so many things, the combination of parameters and settings can become unmanageable, taking weeks and even months of work by the company employees to find the best values for each new product. Therefore, the ISP tuning process is one of the bottlenecks in the transition of a smartphone from the factory to the market.

The main problem with the parameter tuning of the ISP is that, in many cases, it completely involves manual labor performed by different professionals to accomplish it, from photograph experts who analyze the quality and feel of the camera to the programmers who prepare and build the

The associate editor coordinating the review of this manuscript and approving it for publication was Gustavo Olague.

libraries for the camera. It is an iterative process between these professionals that usually starts by defining an appropriate scenario for the tuning and analysis, such as a test chart to obtain distinctively objective values by metrics or a still-life image to acquire a desirably pleasing feeling for most people. Then, the professionals start to tune the values by starting with the factory values or those from previous models, such that the libraries have to be compiled and loaded onto the device. Subsequently, the scenario is photographed by the programmers with all the different libraries that they prepared under different values of lighting to check the response of the camera. After all of the needed images are taken, the analysts give feedback and the corrections that they see fit. The whole process continues until there is a consensus, which, as we previously mentioned, can take weeks or months.

Some research papers have been published in the field of ISP tuning. The work that can approximate the problem posed in our proposal is that of Nishimura *et al.* [13]. An ISP has a pipeline architecture composed of different dedicated hardware blocks that execute a given reconstruction algorithm. The algorithm used by Nishimura *et al.* is a nonlinear optimization algorithm based on Nelder-Mead Simplex [14] and Subplex. Unlike the work presented in this article, in [13], it focuses on the optimization of a limited set of parameters (3 or 4 per block), while the number of parameters sought by our work is much higher, as we will see in the experimentation section. The search for an optimal result in a multidimensional search space is a problem of great complexity. As we will see later, the process of evaluating a possible solution requires more time than other problems, so it is necessary to arrive at a good solution with the minimum number of evaluations. Another work related to the ISP tuning process, in this case focused on advanced driver assistance systems (ADAS), is the study carried out by Yahiaoui *et al.* [15] from Valeo. In their experimental work, the authors demonstrate the difference of tuning the ISP for a commercial camera that seeks the image quality with respect to the subjective appearance of the human eye, compared to the tuning of an ISP whose system aims to improve the image processing algorithms. The work shows how the accuracy of people detection can be improved by tuning the ISP sharpening parameters. A revealing aspect of their work is that they indicate that the tuning process improves the performance of the computer vision algorithms, but they do not provide an automatic solution to find the best parameters of the ISP, as we will demonstrate in our work. Also in the field of ADAS is the work of Mody *et al.* [16] from Texas Instruments. In this case, the ISP tuning process is carried out by establishing some predetermined ISP parameters (there are four in this case: noise Filter, sharpness, defect correction and contrast) depending on the conditions of the scenes being displayed. Depending on the combined conditions of analog gain, exposure time and color temperature, the parameters (initially preset) to be used by the ISP are determined. Although their work is an adaptive tuning according to the conditions of the capture of the images, the authors depart from the purpose of our work in that they automatically search the ISP parameters that allow the capture of the images with the best quality.

Bioinspired techniques that use a metaphor of natural evolution have proven to be very useful in addressing optimization problems. All of these approaches are based on the application of two operators, selection and search, which allow exploring and exploiting the information in the search space [17]. The recombination and mutation operators are used as search operators, and for the selection operator, the well-known biological natural selection metaphor is applied to make it more likely to survive the most adapted solutions; i.e., the solutions that best solve the problem will transmit their achievement to the next generation.

Computational evolution techniques have been used to solve problems in different areas. Within the area of computer vision, different works make use of these techniques. In [18], different works can be found that are related to the application of evolutionary algorithms (EAs) in computer vision problems, such as the accurate modeling of image features, an intelligent approach for three-dimensional reconstruction, or multiobjective sensor planning for accurate reconstruction. The main techniques, referred to as EAs, are genetic algorithms, genetic programming and evolution strategies. Differential evolution (DE) proposed by Storn and Price [19], [20] has emerged as an EA technique with the objective of improving the efficiency of the rest of the techniques in the search for the global optimum with the least number of parameters possible. Only 3 parameters need to be specified: the size of the population, the crossover rate (these parameters are in common with the rest of the EA techniques) and a parameter specific to the DE technique called the scale factor. The differential feature of DE versus other EA techniques is found in the self-referential mutation property. That is, the scale factor allows an automatic and gradual adaptation on all the parameters of the solution vector proportional to the dispersion of each one [21], [22].

Of course, similar to all EA techniques, the approach has the limitations expressed in the NFL (no free lunch) theorem, and it has been described that DE has a great capacity to efficiently explore the search space and find the region in which the global optimum exists, but it is more inefficient in exploiting solutions to refine the result [23]. For this reason, DE will be applied in this work to find the region containing the best solution that human operators will subsequently refine manually.

This article presents a solution to the ISP tuning process problem, where the validation of a possible configuration is costly in time, so the priority is to obtain an acceptable solution in a few iterations of search and with a limited population in size, rather than finding the best solution. The fine-tuning process can be carried out manually by a camera tuning engineer and without having to involve numerous trial and error tests, which, in practice, are usually very time-consuming tasks (several weeks and even months). In this way, the whole process (Figure 1) is based on a first phase where several hundred images are analyzed automatically, finding the most

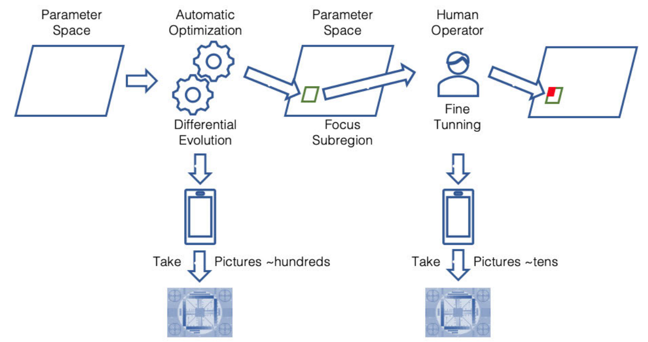

FIGURE 1. **Complete process for ISP tuning.**

promising region quickly. In a second stage, the engineer with a few tens of images performs the fine-tuning. In the first section of the paper, we will describe the parameters related to the quality of the image that will help us understand the quality objectives that we want to obtain. Then, the DE algorithm that is developed for optimizing the ISP parameters is described. Finally, the results obtained in different experiments will be presented.

II. IMAGE QUALITY

Image quality is defined as a set of factors that reflect the level of accuracy of the system to capture, process, store, compress, transmit and display the signals that form an image. Another definition would be the "weighted combination of the visually significant attributes of an image" [25]. The key difference is that the second definition places more emphasis on evaluation through the perception of attributes that make an image attractive to a human being. Some characteristic attributes and elements that define image quality are the following:

- Sharpness: Determines the amount of detail that an image transmits. It is perceived through the definition of the edges of the image. You can increase the perception of sharpness through edge enhancement, but if it becomes excessive, it becomes an embossed envelope of edges and you begin to see halos.
- Noise: Random variation of the density of the image, visible as a film granulate or as variations of pixels in digital images.
- Dynamic Range: The range of light levels that a camera can capture. This relates to the smallest and the largest amount of light level that can processed. In case there is information that cannot be processed because it is outside of that range, it is depicted as noise.
- Tone Reproduction: It is the relation between the luminosity of the scene and the brightness reproduced in the image. This tries to represent light in a scene by balancing the brightness and intensity of colors in the elements of the image.
- Contrast: It is the slope of the curve of the tonal reproduction. High contrast means less intermediate values between tones, whereas a low contrast increases those values by reducing the amount of variation, leading to a loss of quality incurred by both extremes.
- Color Accuracy: Is the measure of color changes, saturation and effectiveness of white balance.
- Distortion: It is an aberration that causes straight lines to curve in the image.
- Vignette: It is the gradient of light at the edges of an image, caused by the difference in light received at the different points of the lens (being convex normally, the center of the lens receives more light, especially in wide-angle cameras).
- Exposure: The amount of light per unit area received in the sensor, determined by the shooting speed, the aperture of the lens and the light of the scene.
- Chromatic Aberration: It is an aberration produced by the lens that causes the convergence of colors in the same point, rendering the inability to focus them correctly.
- Lens Flare: It is a phenomenon in which a ray of light is dispersed and captured in the lens, causing brightness and reflections between the lens and the elements of the camera, generating noise, loss of detail and color in the image.
- Artifacts: Different software processes can cause distortions in the image due to the compression and transmission of the image, causing loss of detail through halos or noise.

Although several of these attributes are quantifiable, not all follow standardized measures, since several are subjective to the observer.

A. RESOLUTION AND MODULATION TRANSFER FUNCTION

Before tackling the oversharpening of edges and the modulation transfer function (MTF), we must explain the concept of resolution. The resolution is the amount of detail captured in the image (as opposed to the sharpness, which is the amount of detail perceived), measured by the accuracy of capturing the smallest details possible. The resolution is usually measured by observing the number of discernible lines in a vertical section (lines per millimeter, ln/mm) from a photograph to a test chart (see Figure 2).

One problem with this is that the ability to discern lines also depends on the ability of the observer. In this way, the MTF can be used to determine the resolution. The idea of this is that the MTF allows us to calculate the contrast, which describes the detail in the lines. The MTF equation (Equation (2)) is derived from the sinusoidal pattern of the contrast $C(f)$ (Equation (1)) at a spatial frequency f (the spatial frequency is the distance of the elements of a pattern [26]), where:

$$C(f) = \frac{V_{max} - V_{min}}{V_{max} + V_{min}} \tag{1}$$

for luminance (intensity) V

$$MTF(f) = 100\% \times \frac{C(f)}{C(0)} \tag{2}$$

normalizes MTF 100% at low spatial frequencies.

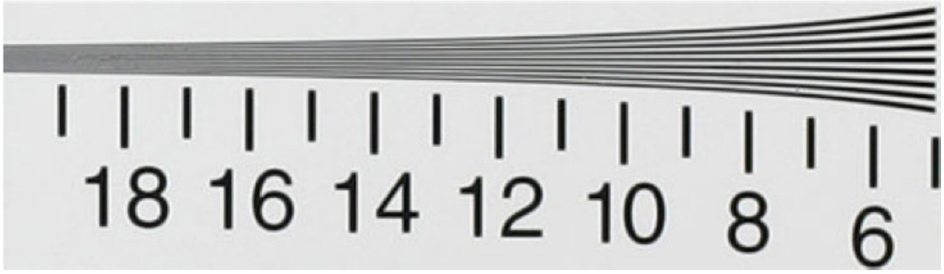

FIGURE 2. Imatest SFRPlus test chart [24].

Obviously, the spatial frequency is related to the understanding that, in a low-frequency space, the lines to be evaluated are smaller, so the closer it is to 0, the less contrast there is, and therefore, fewer lines can be identified. The best case is when the MTF is equal to 50%, which indicates that it is visible, and below 20% – 10% is the case when it is considered indistinguishable.

FIGURE 3. Slanted edges from Imatest ISO-12233 extract [24].

By the standard established by the CPIQ (1858-2016 - IEEE Standard for Camera Phone Image Quality Standard), resolution is no longer measured with the bar system, but rather with slanted edges and the MTF, and the slanted edges can be seen in Fig. 3. This is because of the advantages it offers; it does not depend on the distance with the chart, it has reduced space so it can fit on different charts, and there is no need of manual counting of the visible lines; thus, it is capable of being automated.

B. SIGNAL-TO-NOISE RATIO AND VISUAL NOISE

Noise is a very important factor when determining the quality of an image, given that noise is the amount of random signal variations for each pixel. It is usually measured by means of the SNR function, the signal-to-noise ratio, where the amount of noise is expressed through the standard deviation of pixels measured in decibels (dB). However, we are going to focus on the measure of the visual SNR, or visual noise, consisting of the amount of noise that can be perceived by a human. This measure is calculated through a series of patches in the range of grays in the test chart (Fig. 4), taking the measurements from three points of view, where each one is specified through its height and viewing distance. In this way, the visual SNR is calculated with a series of complex formulas specified in the IEEE CPIQ P1858 of 2017 [25], where there are different calculations that include the effects of the human vision system.

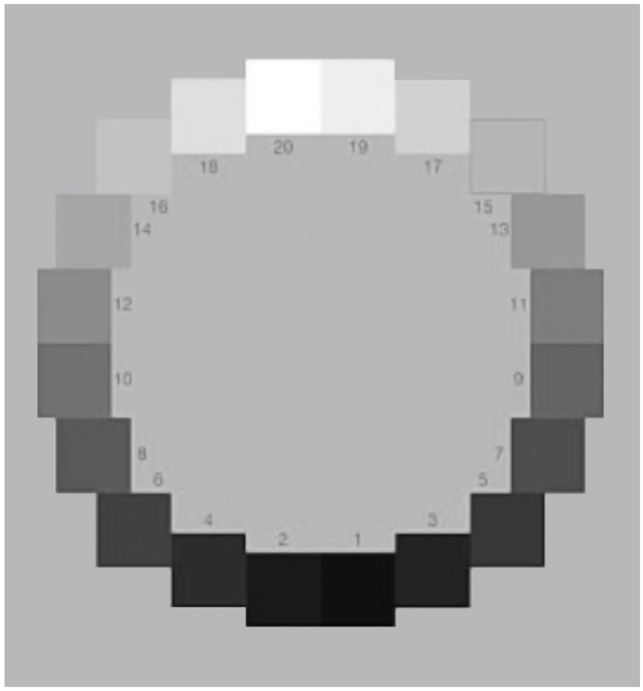

FIGURE 4. Gray patches from Imatest ISO-12233 extract [24].

C. ACUTANCE AND SUBJECTIVE QUALITY FACTOR

The SQF (subjective quality factor), is a measure of the perceived sharpness of an image through a function that considers the height of the image and the distance of visualization of it. It tries to describe the subjective perception of a spectator.

The SQF of an image is measured by analyzing a photograph taken on a test chart; specifically for this project, the ISO-12233 for SFRPlus has been used in this work (see Figure 5). For the analysis, a series of regions of interest (ROIs) distributed by the image are determined, where the SQF values are calculated and distributed in three regions that are weighted according to their distance to the center of the image, with the center being the most significant region [25].

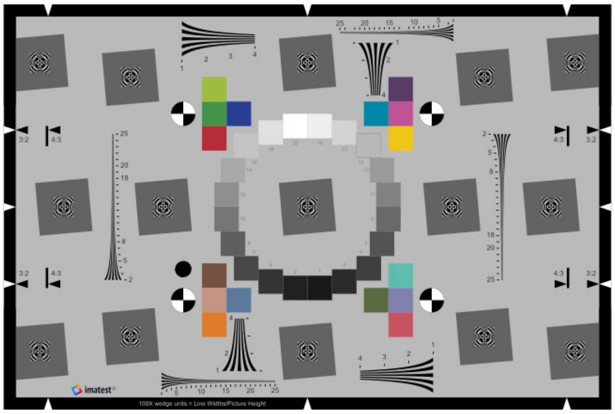

FIGURE 5. Imatest ISO-12233 test chart for SFRPlus analysis [24].

The regions of interest that are chosen from this chart are the sides of the gray squares by measuring the sharpness of the edges and taking the average of each region. The SQF values are intended to be proportionally linear to perception, with an SQF difference of 5 being the perceptible amount of sharpness change. This means that a viewer may not notice the difference in sharpness between an image with an SQF of 88 and an SQF of 90 but will notice the difference in images between 88 and 93. This brings us to the values of the acutance (see Table 1)

TABLE 1. Acutance values.

A+	A	B+	B	C+	C	D	F
94 – 100	89 – 94	84 – 89	79 – 84	69 – 79	59 – 69	49 – 59	Under 49

The ideal values of acutance are from 94–100, as indicated in the table (see Table 1), but an image with much noise or sharpening can surpass the 100 score despite not having an adequate quality. The reason is that the calculus of the SQF (Equation (3)) takes the MTF value into account. This means that since the approach can find regions filled with high contrast frequencies due to the noise, it obfuscates the measure, making it believe that the image is properly sharpened. Next, its value calculation is expressed [27]:

$$
\begin{aligned}
SQF &= K \int_{\infty}^{0} CSF(f) \cdot MTF(f) \cdot d(\ln f) \\
&= K \int_{\infty}^{0} \frac{CSF(f) \cdot MTF(f)}{f} \cdot df
\end{aligned} \tag{3}
$$

where:

- CSF is the contrast sensitivity function of humans; CSF *(f)* is close to 0 for $f > 60$ cycles/degree
- MTF *(f)* is the modulation transfer function.
- $K = \frac{100\%}{\int CSF(f) d(\ln f))} = \frac{100\%}{\int \frac{CSF(f)}{f} df}$ is the normalization constant: SQF is equal to MTF *(f)* with a constant value of 1.

To calculate the CSF *(f)*, it is necessary to present the spatial frequency (*f*) in cycles / degree (Equation (4)), which is initially calculated in Imatest as cycles/pixel, so that:

$$
f(cycles/degree) = \frac{\pi n_{PH} d f(cycles/pixel)}{180 PF} \tag{4}
$$

where:

- n_{PH} is the number of vertical pixels.
- d is the viewing distance.
- PF is the height of the image in cm.

III. DIFFERENTIAL EVOLUTION

Differential evolution (DE) is a stochastic search algorithm, which belongs to the set of evolutionary algorithms, based on recombination, evaluation and selection of individuals. It was designed with the aim of optimizing continuous nonlinear and nondifferential functions [19], [20], [28]. In our work, DE was chosen over other evolutionary algorithms since DE does not need large populations or many generations to reach a solution. This aspect is important due to the time factor when carrying out the experiments since the process of taking photographs can take many generations and individuals and takes a long time. The strategy of the algorithm is that, for each individual, a random selection of a set of different parents is made, and a random recombination between them forms a new individual, which in turn receives a random set of mutations. The new individual is evaluated, and the best is selected between the new and the old.

```
Algorithm 1 Differential Evolution
Data: Population Size (N), Problem Size (X), Mutation
      Factor (F), Recombination Factor (Cr)
Result: Best solution (x_Best)
Population ← Initialize_Population (N);
Evaluate_Population (Population);
X_Best ← Get_Best (Population);
while ! Stop_Criteria do
    New_Population ← 0 ;
    for i < N do
        v_i ← New_Individual (x_i, N, F, Cr) ;
        if x_i ≤ v_i then
            New_Population ← v_i;
        else
            New_Population ← x_i;
        end
    end
    Population ← New_Population ;
    Evaluate_Population (Population);
    X_Best ← Get_Best (Population);
end
return S_Best
```

In Algorithm 1, a scheme of the general pseudocode of the differential evolution is shown, where the inputs, the output and the basic operation are described. The entries are composed of the following:

- Population Size: The number of individuals with whom the algorithm will work. DE does not need a large number of individuals to reach a solution, but if it is too small, it is likely to stagnate or take a long time to converge; however, its appropriate size depends on the size of the problem.
- Problem Size: It is the space in which the problem is found. It is the number and type of variables with their ranges of possible values.
- Mutation Factor: It is a factor normally between [0, 2] that controls the amplification of the difference between two of the parents to generate new parameters during the creation of a new individual in a generation.
- Recombination Factor: It is a factor between [0, 1] that controls the probability that the donor's new value will be applied to the new individual.

In Algorithm 1, we can also find the use of the following characteristic functions:

- *Initialize_Population*: This involves generating a new population randomly with a number of individuals equal to the population size.
- *Evaluate_Population*: To evaluate each individual of the population, it is necessary to have an objective value that is taken from some type of criterion pertaining to the problem (the value of some function through the parameters, for example), which allows us to calculate the error of each individual regarding the target value.
- *Get_Best*: It is about obtaining the individual that best meets the assessment. Depending on how the value of the evaluation is interpreted, minimization or maximization is performed.
- *New_Individual*$(v_{i,j})$: For a better understanding, the pseudocode is shown in Algorithm 2. First, different random individuals are selected from each other and from the original individual, called parents (p_1, p_2, p_3). Once the three parents are obtained, the values (j) of the original individual (x_i) are modified, with a probability determined by the recombination factor (Cr), through the following function (see Equation (5)):

$$v_{i,j} \leftarrow p_{1,j} - F \times (p_{2,j} - p_{3,j}) \tag{5}$$

  In this way, the new values are dependent on the parents, but by mutating, they can empower the individual regardless of their quality.

It should be noted that the algorithm always approaches a better solution, never a worse one. It may happen that, if there is little diversity among the population, it will stagnate and not progress for many generations since it will have reached a point where it can only advance through random enhancements of the mutation. Normally, at this point where the entire population has little difference with the best individual, it is considered that it has converged to that solution.

IV. PROBLEM STATEMENT

In the case of our experimentation, we are going to work with the ISP Qualcomm Spectra 160, which includes the processor of the smartphones with which we work (Snapdragon 660). This ISP has been designed to support quality photography through noise reduction, low-light algorithms, and computational camera innovations. The ISP has a set of parameters that must be specified for each model of the mobile device to be manufactured. Therefore, our goal is to find those ISP parameters that obtain an improved image quality for a particular model of the smartphone.

Algorithm 2 *New_Individual*

```
Data: Individual (x_i), Population Size (N), Mutation
      Factor (F), Recombination Factor (Cr)
Result: New Individual (v_i)
do
  | p_1 ← Random_Individual (Population) ;
until x_i ≠ p_1;
do
  | p_2 ← Random_Individual (Population) ;
until x_i ≠ p_2 and p_1 ≠ p_2;
do
  | p_3 ← Random_Individual (Population) ;
until x_i ≠ p_3 and p_1 ≠ p_3 and p_2 ≠ p_3;
for j in x_i do
  | if random() < Cr then
  |   | v_{i,j} ← (p_{1,j} + F × (p_{2,j} − p_{3,j}) );
  | else
  |   | v_{i,j} ← x_{i,j} ;
  | end
end
return v_i
```

We will now describe the process of obtaining the ideal parameters:

1) Starting with the algorithm, once we have the parameter of the ISP for each individual, we generate and compile the libraries for the camera.
2) Then, the library is loaded onto the camera, and the phone is rebooted to catch it.
3) After the reboot, we take a photograph with the library.
4) Then, we repeat the load, reboot and take the photograph for each of the libraries.
5) Once we have all the images, we analyze each of them with Imatest to obtain the quality metrics and store the results.
6) We compare the quality of the new individuals with their correspondent of the previous generation and keep the best. Since we store the results of previous individuals, we do not need to analyze old photographs again, just compare the stored values.

In terms of time, there are great variations in the amount of time taken by each step, where the fastest is to generate all the libraries for the generation, which takes up to 4 seconds; then, taking a photograph takes approximately 5 to 15 seconds each; finally, the slowest step involves analyzing the photographs, and this has usually taken up to 30 seconds each. The time taken for the overall process would be approximately 10 to 15 minutes per generation, always considering that if there are more individuals, the time for each generation is increased since there are more photographs to take and analyze, as these are the largest bottlenecks. The outline of the described process is shown in Figure 6.

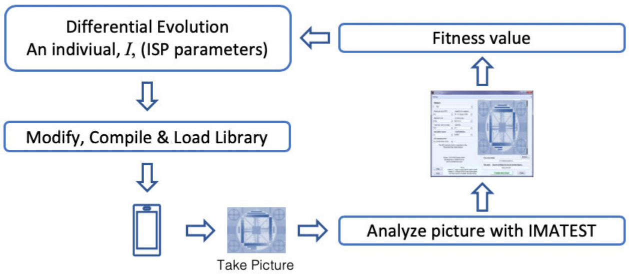

FIGURE 6. **Scheme of the optimization process.**

Each of the elements of this optimization process will be described in more detail in the following sections.

A. ISP PARAMETERS AND RESTRICTIONS

Since the ISP contains many modules for the image processing, each of them dedicated to a different aspect of image quality, we have focused on those related to the processes of sharpening and noise reduction to reduce the size of the problem so that it can be better addressed. The optimization could be done with other parameters of the ISP; these two have been chosen because they are two that are mostly contradictorily processed. For contrast enhancement, contrast effects are usually accentuated so that some amount of noise is always generated collaterally, while blur reduction techniques are usually used to increase the homogeneity of pixels, which results in a loss of detail at the edges. However, this process could be repeated with other parameters.

The ISP library parameters that we are going to optimize belong to the ISO 800 section, whose restrictions are the following:

- Denoise Scale Y: It is a vector of 4 decimal values between [1, 10]. It serves to reduce the noise of the luminance channel. Each value affects a different frequency, and the higher it is, the greater the effect.
- Denoise Scale Chroma: It is a vector of 4 decimal values between [1, 20]. It is used to reduce chroma channel noise. Each value affects a different frequency, and the higher it is, the greater the effect.
- Denoise Edge Softness Y: It is a vector of 4 decimal values between [1, 15]. It serves to soften the edges and reduce the noise of the luminance channel even more. Each value affects a different frequency, and the higher it is, the greater the effect.
- Denoise Edge Softness Chroma Y: It is a vector of 4 decimal values between [1, 25]. It serves to soften the edges and reduce chroma channel noise even more. Each value affects a different frequency, and the higher it is, the greater the effect.
- Denoise Weight Y: It is a vector of 4 decimal values between [0, 1]. It serves to eliminate details of the luminance channel and reduce the noise even more. The lower the value is, the more effect that is applied.
- Lut 1: It is a vector of 24 decimal values between [0, 7.95]. It is used to indicate the intensity of the horizontal edge enhancement with a noise threshold. It generates an upward curve to reduce small amounts of noise at the edges.

Although they have not been included, there are a number of general guidelines that are usually met, including that the parameters that affect chroma should have values with very little difference between one or the other or that the Lut should form an ascending curve, but we have decided not include them as restrictions to check if they are really necessary or not to obtain good results.

TABLE 2. **Default values of the ISP library.**

ISP LIBRARY PARAMETERS	VALUE
Denoise Scale Y	[3.0, 3.0, 4.0, 4.0]
Denoise Scale Chroma	[15.0, 15.0, 15.0, 15.0]
Denoise Edge Softness Y	[2.0, 2.0, 3.0, 3.0]
Denoise Edge Softness Chroma	[15.0, 15.0, 15.0, 15.0]
Denoise Weight Y	[0.0, 0.0, 0.0, 0.0]
Lut	[0.0, 0.0, 0.1902, 0.3756, 0.5514, 0.7134, 0.85728, 0.97956, 1.077, 1.14732, 1.18848, 1.19976, 1.18068, 1.13172, 1.05408, 0.94992, 0.94992, 0.94992, 0.94992, 0.94992, 0.94992, 0.94992, 0.94992, 0.94992]

The default values of the ISP library are depicted in Table 2:

A picture taken with these default parameters is shown in Figure 7. At first glance, you can see that this picture is quite clear and has little noise. However, when a 100% zoom is made, as seen in Figure 8, there is a certain amount of oversharpening of edges, perceived with a slight halo, but indeed with very little noise, just a slight chroma noise in the dark square.

B. IMATEST MASTER

Imatest Master is an image quality analysis program that is part of Imatest. With this program, we will be able to analyze the test chart that has already been shown in Figure 3 and take out the necessary values for the evaluation in different

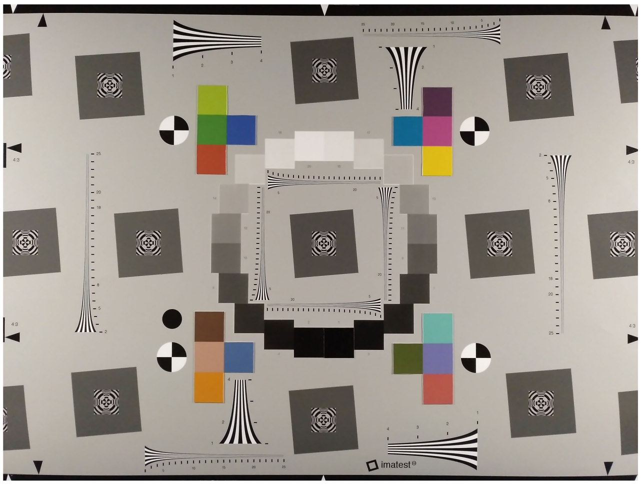

FIGURE 7. Photograph of ISO-12233 with default values [24].

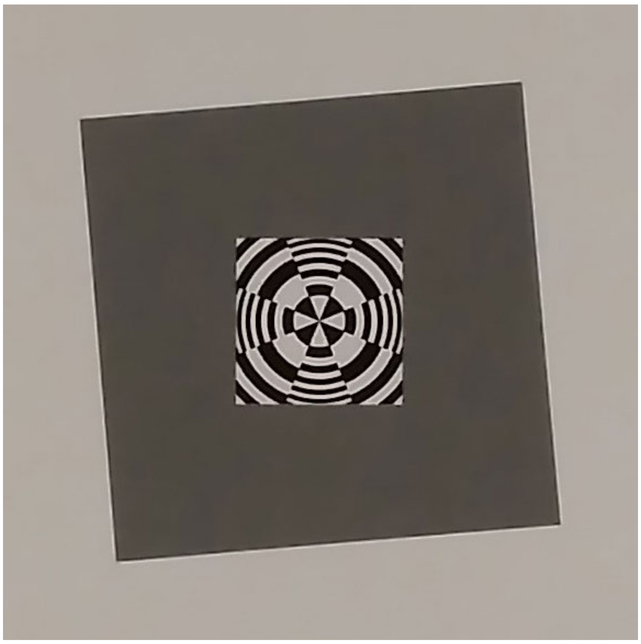

FIGURE 8. Zoom of Figure 7.

output formats. The program allows us to generate diagrams, Excel tables and JSON files with the results, but for greater convenience and speed, we will only take into account the results stored in the JSON files, and we will not generate any of the other files during the process to obtain a solution, only as part of the validation of results. It should be noted that Imatest Master is a program primarily designed for manual analysis and therefore has a graphic interface designed for it. However, Imatest Master contains a dynamic library called Imatest Push Interface, which allows the user to make use of Imatest through C ++ so that even though the user interface can continue to be run, the user can send them to analyze images automatically.

The Imatest application returns a set of parameters that measure the quality of an image. Of all the measures provided by JSON, we will focus on three indexes:

- SQF: It is a vector of 36 values, where each value corresponds to a different distance. We are interested in a viewing distance of 30 centimeters, and we will choose the value 11 of the vector.
- OversharpeningPCT: It is a vector with the percentages of oversharpened edges in each region of interest of the test chart. We will take the average among all and try to take it to the point that interests us.
- SNR Visual Noise: It is a vector that contains the amount of noise measured in the gray range patch in the center of the test chart. We take the average of the centrals since those of the extremes correspond to the blacks and whites and can generate problems when calculating the average.

C. DIFFERENTIAL EVOLUTION

The algorithm shown in section III (Algorithm 1 and 2) is a version with a slight modification of the standard algorithm with a binomial version of Crossover. In the standard algorithm, when a new individual (solution) is created, it is evaluated to see if it is better than the previous solution. In our problem, to reduce the time between generations, it is first instantiated and compiled all libraries of the new individuals. Then, after all are created, it is evaluated and compared each new individual with its previous iteration and then decide which is the best. This small adjustment saved us a considerable amount of time since the libraries could be compiled all at once and the images could be analyzed as batches.

In order to fine-tune the parameters of the algorithm, the population size and the number of generations, some measurements of the behaviour of the algorithm were made by modifying the population size. The Ackley function was used [29], a non-convex, scalable function with many local minima with a global optimum value at 0.

We estimate that the parameter search performed to have an approximation to the optimal region in Ackley's function could be suitable for the ISP parameter adjustment problem. We made 100 runs of the modified DE algorithm (DEm) and the standard DE algorithm (DEs) with populations of 5, 10, 15, 20, 25, 30 and 40 individuals for 100 generations. Figures 9, 10, and 11 show the boxplot of the best individuals for Ackley's function with 5, 10 and 44 dimensions, respectively. This last value matches the dimensionality of the ISP setting. It can be seen that for low dimensions both DEm and DEs have a similar behavior. It agrees, as expected, with the worst result for the population of 5 individuals. For dimension 44, it can be seen that DEm improves the DEs by approximating the region in which the global optimum is found. Specifically, the best result is produced from a population of 15 individuals. In the tests carried out in the experimental section, populations of 15 and 30 individuals are selected. These results validate the modification of DE and justify the population size.

For the search of the parameters that satisfy the quality conditions of an image, we will use the evolutionary differential

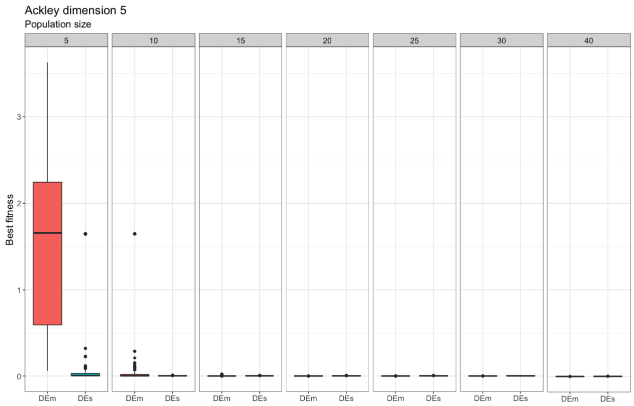

FIGURE 9. **Modified vs standard DE performance in Ackley (dim. 5).**

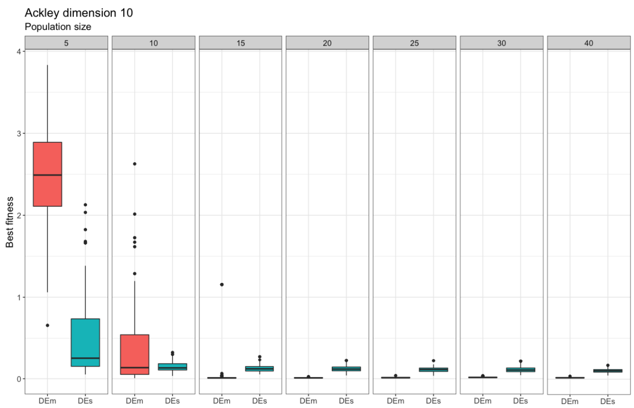

FIGURE 10. **Modified vs standard DE performance in Ackley (dim. 10).**

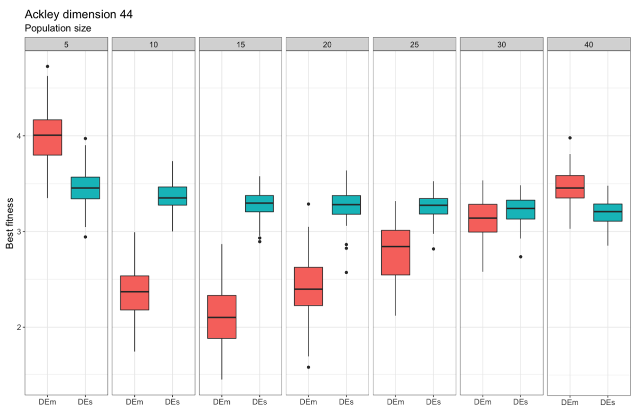

FIGURE 11. **Modified vs standard DE performance in Ackley (dim. 44).**

algorithm described in Algorithm 1. At the beginning of the search, we have a set of individuals, which describe certain values for the ISP parameters. Initially, they will take a random value. The objective is to find the set of ISP parameters that allow obtaining an image whose quality metrics (SQF, OversharpeningPCT (OV) and SNR Visual Noise (VN)) approach initially defined target values. Photographs with these parameters will be taken and their quality will be assessed using the Imatest application. The fitness function of each of the individuals is described as the deviation of the values obtained in Imatest from the target values. For instance, the deviation value of the SQF image quality attribute (Dev_{SQF}) is calculated by applying Equation (6).

$$Dev_{SQF} = \left| 1 - \frac{|SQF_{target} - SQF_{obtained}|}{SQF_{target}} \right| \times 100 \quad (6)$$

where SQF_{target} is the ideal value to be obtained and $SQF_{obtained}$ is the value obtained by a given individual. Similarly, we will obtain the values for Dev_{OV} y Dev_{VN}, or any other image quality attribute to be optimized.

Once we have obtained these deviations, the fitness function is in the form of the linear regression function of Equation (7).

$$fitness = Dev_{SQF} \times P_1 + Dev_{OV} \times P_2 + Dev_{VN} \times P_3 \quad (7)$$

where P_1, P_2 and P_3 are weighting values. During the research, those values were determined by the head engineers from BQ based on the results, so it was an iterative process. In the end, those parameters mark the relevance of the different quality measures, so, for example, if what you want is to value more the sharpness over the visual noise, you would increase the SQF percentage (P1) on the final measure. The values P_1, P_2 and P_3 are established by the team of expert engineers, thanks to their experience. These values can be used by them when tuning the ISP of other camera models.

In addition, to penalize and further restrict certain values, we place them in a minimum range to calculate their deviation:

- The SQF must be less than 120 to be taken into account; otherwise, its deviation will be worth 0.
- The oversharpening of edges must be less than 100 to be taken into account; otherwise, its deviation will be worth 0.
- The visual noise must be less than 50 to be taken into account; otherwise, its deviation will be 0.

The evaluation cycle will be carried out according to the scheme in Fig. 6 until the stop condition is met. In our case, the stop condition is a specific number of generations.

Finally, the quality of solutions should be the final point of the optimization procedures, and in this case, we have an evaluation of experts: engineers who optimize the parameters for each type of terminal. The solution is that the algorithm finds the starting point for these engineers, and the validation of these solutions is given by the subjective opinions of the experts. If solutions generate a probabilistic distribution defined by the average and deviation, it is not so representative here because the problem is not to find the "optimal solution"; rather, the problem is only to find the start region that is near the optimal solution and thus begin the engineering work.

V. DISCUSSION OF RESULTS

A. TESTS PERFORMED

The tests have been carried out in a dark room, where the only illumination came from the two focuses centered and oriented at 30° with respect to the test chart. The photographs were taken at 45 cm to focus only the 4:3 section of the test chart to facilitate the analysis with Imatest. In the following paragraphs, we will discuss the tests performed, where the objective values of the tests were changed, in a search for better results. In these tests, a recombination factor of 0.7 and a mutation factor of 0.5 were established. This decision was made in order to generate individuals with exaggerated modifications, and since there are many parameters, when reaching an advanced point in the generations, the modifications should not be so radical due to the sensitivity of the modifications.

B. TEST1

This test was performed with a population of 15 individuals, with the following targets:

- SQF: 100
- Oversharpening of edges: 5
- Visual noise: 35

In addition, the objective function was weighted as:

- The deviation of SQF by 20% of the score
- The deviation of the oversharpening of edges by 35%
- The deviation of visual noise by 45%

These weights were chosen after realizing that the sharp edge envelope greatly influenced the SQF, and the visual noise ended up being set aside in a more homogeneous distribution. This test has required 1, 290 photographs, which took an approximate total time of 15 hours.

In Fig. 12, the evolution of the generations through the average of the scores of the individuals and the best individual is depicted.

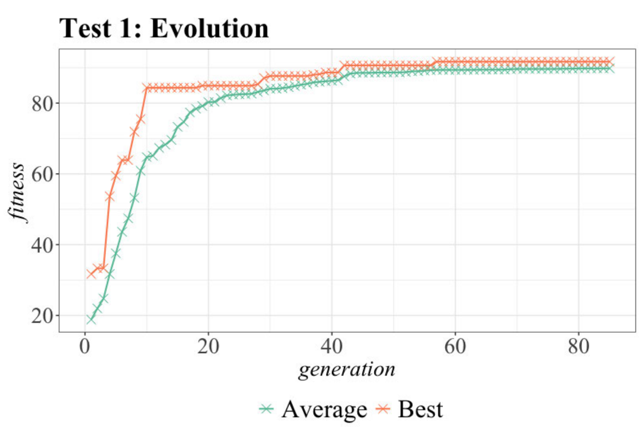

FIGURE 12. Evolution of the generations of Test1.

We can verify that the algorithm begins to converge approximately from generation 55 and finishes doing so at approximately generation 80.

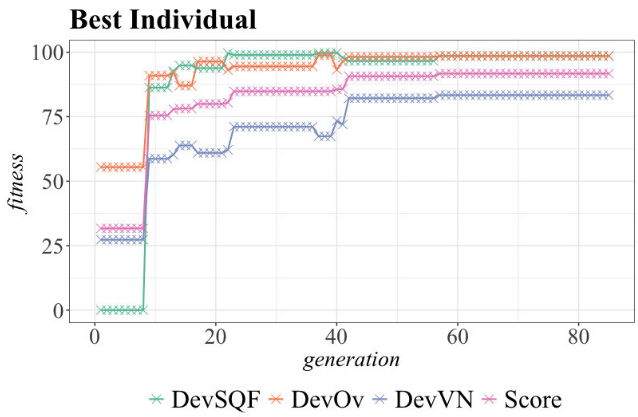

FIGURE 13. Evolution of the best final individual of Test1.

In Fig. 13, we can see the evolution of the best final individual throughout the generations. This individual has not been the best in all generations, but it allows us to obtain an idea of how an individual progresses. In this case, we can verify that there was very sharp progress from generation 8, where the oversharpening dropped enough to allow the value of the SQF to exceed the threshold and be considered mainly in the function. We can also verify that there are slight alterations regarding what values are enhanced in each generation. For instance, in generation 38, it can be seen that part of the visual noise is exchanged for better edge sharpening, but only because the sum of both provided a better score. Likewise, we can see that the criterion that does not reach the objective value is the visual noise, which indicates that the objective value is not entirely attainable or compatible with the rest of the criteria. This observation is confirmed when looking carefully at the values of visual noise of the other individuals that do not reach the target.

In Table 3 and 4, the quality values achieved by the best individual and their ISP parameters are depicted.

TABLE 3. TEST 1. Quality values obtained of the best individual of Test1.

IMAGE QUALITY ATTRIBUTES	VALUE
SQF	101.4
OvSha	3.52583333333
VNoise	29.1760833333

Comparing the values of these parameters with the default values (Table 2), we can observe that there is a greater intensity in the majority of noise reduction parameters and that, in addition, it does not follow the same type of distribution where the majority of values of the same vector are the same, although there is a certain tendency for them to be close to each other. In the Lut, we have that the function described is quite abrupt but moderately increasing. As we will see, this property translates to a certain amount of the sharp envelope. In Fig. 14, which corresponds to the photograph taken with this library, it can be verified that it actually provides a

TABLE 4. TEST 1. ISP parameters of the best individual of Test1.

ISP LIBRARY PARAMETERS	VALUE
Denoise Scale Y	[9.683125, 2.685479, 5.580432, 8.134182]
Denoise Scale Chroma	[15.142409, 6.550038, 8.434523, 9.463016]
Denoise Edge Softness Y	[9.541614, 1.0, 7.053057, 9.950132]
Denoise Edge Softness Chroma	[19.722641, 25.0, 14.870583, 20.919238]
Denoise Weight Y	[0.0, 0.091192, 0.0, 0.108497]
Lut	[0.0, 0.0, 1.473661, 0.146923, 0.0, 1.344536, 0.437417, 0.10109, 2.607141, 2.176709, 0.0, 0.327008, 1.122977, 5.577412, 7.722511, 0.0, 1.945425, 5.223309, 7.32656, 3.262385, 0.576531, 7.559592, 0.0, 0.0]

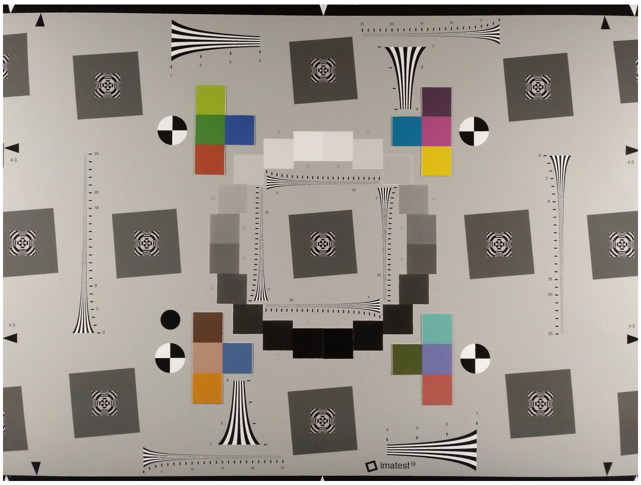

FIGURE 14. Photograph of the best individual of Test1.

fairly high sense of sharpness, with very little noise, which corresponds to the results in the evaluation criteria.

C. TEST2

This test was performed with a population of 30 individuals, with the following targets:

- SQF: 100
- Oversharpening of edges: 5
- Visual noise: 35

In addition, the objective function was weighted as:

- The deviation of SQF by 20% of the score
- The deviation of the oversharpening of edges by 35%
- The deviation of visual noise by 45%

In Fig. 15, the evolution of the best individual and the average of individuals in each generation is shown.

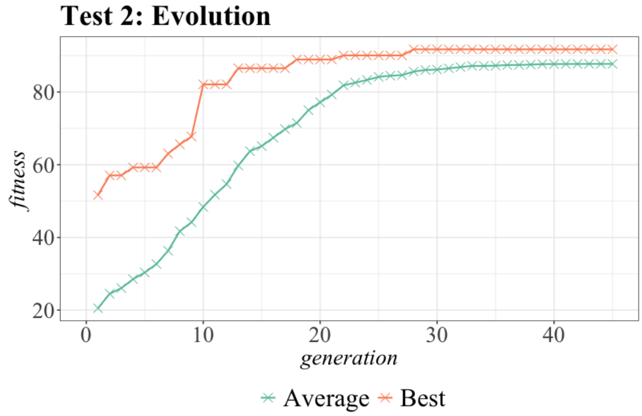

FIGURE 15. Evolution of the generations of Test2.

This test is subject to the same conditions as in Test1, except that there are 30 individuals, so we can see that, being a larger population, it has taken less time to converge; however, in turn, it can also be seen that the progress of the average is softer. It can be seen that it begins to converge from generation 27 and that from 35 there is very little variation. In generation 45, the average value is 87.73, while the best value is 91.74. Compared with the previous test, we can see that the value of the best individual is very similar, while the value of the average is slightly lower because there is more variety.

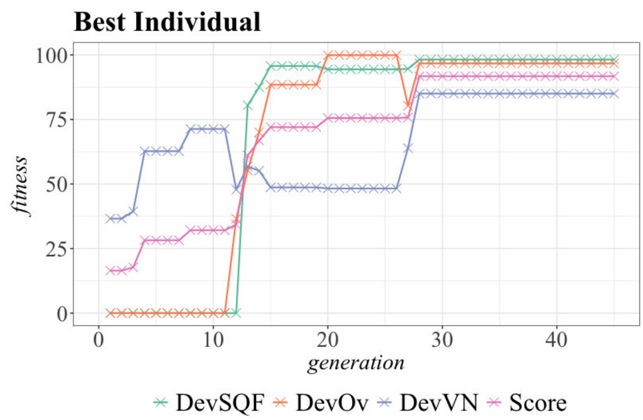

FIGURE 16. Evolution of the best individual of Test2.

In Fig. 16, the evolution that the best final individual has followed throughout the generations can be observed. This individual has not been the best in all generations, but it allows us to obtain an idea of how an individual progresses. In this case, we can verify that there was very sharp progress from generation 12, where the oversharpening dropped enough to allow the SQF value to exceed the threshold and be considered in the function, in the same way as the best individual of Test1. We can observe that, in this case, generation 27 was reached, and part of the value of the oversharpening was lost in exchange for achieving a better noise reduction, but in generation 28, both values were recovered to the maximum reached. Again in this test, it can be seen that the objective value that is not reached is that of noise reduction, so it confirms that it is not an adequate objective value.

In Table 5 and 6, the quality values achieved by the best individual and their ISP parameters are depicted.

TABLE 5. TEST2. Quality values obtained of the best individual of Test2.

IMAGE QUALITY ATTRIBUTES	VALUE
SQF	98.2
OvSha	1.70833333333
VNoise	29.7533333333

TABLE 6. TEST2. ISP parameters of the best individual of Test2.

ISP LIBRARY PARAMETERS	VALUE
Denoise Scale Y	[8.779436, 3.674315, 7.893943, 6.141733]
Denoise Scale Chroma	[14.638331, 16.710903, 1.0, 7.060322]
Denoise Edge Softntess Y	[9.246852, 12.263236, 1.0, 5.439948]
Denoise Edge Softntess Chroma	[1.0, 25.0, 21.213278, 16.521372]
Denoise Weight Y	[0.0, 0.070773, 0.0, 0.0]
Lut	[0.0, 2.099394, 4.17596, 0.0, 0.706986, -0.0, 1.394175, 3.975, 5.243605, 0.0, 7.186879, 0.668851, 0.164072, 4.200143, 0.0, 5.952424, 0.727468, 5.665776, 1.0555, 0.0, 1.171377, 1.073743, 0.934245, 1.786077]

Comparing the ISP parameters of the best individual with the default values (Table 2) and the values of Test2 (Table 6), we can see that again there is a greater intensity in the majority of noise reduction parameters and that, in addition, it follows the same type of distribution as the default values. However, again there is a tendency to have values that are close to each other, although in very different ways than in Test1. In the Lut, we have that the function described is quite abrupt, reaching many peaks. This translates, as we will see in photography, to a special type of edge sharpening with many artifacts and a very increased halo. In Fig. 17, which corresponds to the photograph taken with the parameters of the best individual of Test2, it can be verified that, as indicated by the SQF, it gives a feeling of high sharpness.

This test has required 1, 380 photographs, which took an approximate total time of 16 hours. This result implies that in 16 hours, the same result has been achieved as that in Test1, which required 15 hours; however, the amount of generations

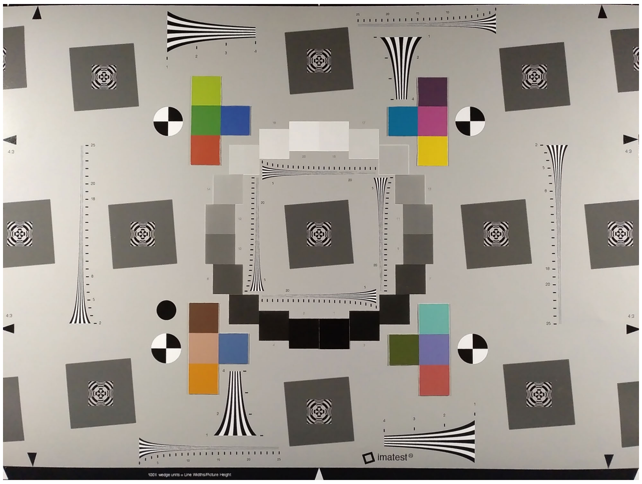

FIGURE 17. Photograph of the best individual of Test2.

needed is significantly less, which leads us to observe that the evolution of individuals is much faster because there is a greater diversity of parameters to work with.

D. TEST3

This test was performed with a population of 30 individuals, with the following targets:

- SQF: 100
- Oversharpening of edges: 2
- Visual noise: 25
- MTF: 0.3

In addition, the objective function was weighted as:

- The deviation of SQF by 20% of the score
- The deviation of the oversharpening of edges by 30%
- The deviation of visual noise by 30%
- The deviation of MTF by 20%

In this experiment, we decided to introduce one more image quality attribute (MTF). We wanted to check the behavior of the optimization when introducing MTF, so we redefined the initial fitness function of (7) by the following function:

$$fitness = Dev_{SQF} \times 0.2 + Dev_{OV} \times 0.3 + Dev_{VN} \times 0.3 + Dev_{MTF} \times 0.2 \quad (8)$$

In Fig. 18, the evolution of the best individual and the average of individuals in each generation is shown.

In Fig. 18, the rapid convergence of the population in the generation from generation 17 is shown. This is the case of the fastest evolution that we have obtained in the tests performed. It can also be observed that, as in Test2, the population growth is smoother due to the number of individuals. In generation 20, the value of the average population is 92.61, while the best individual has a value of 96.13.

Fig 19 shows the process that the best final individual has followed throughout the generations. This individual has not been the best in all generations, but it allows us to obtain an idea of how an individual progresses. In this case, we can

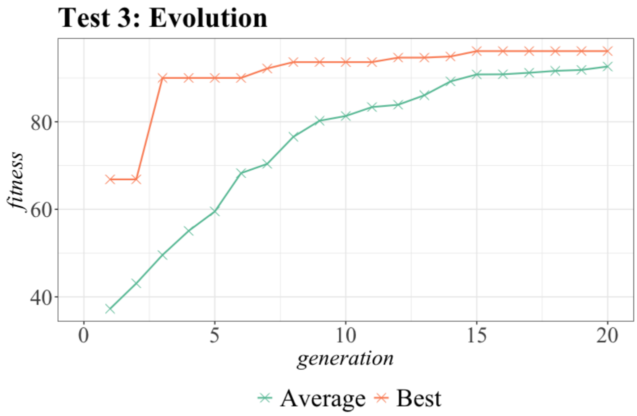

FIGURE 18. Evolution of the generations of Test3.

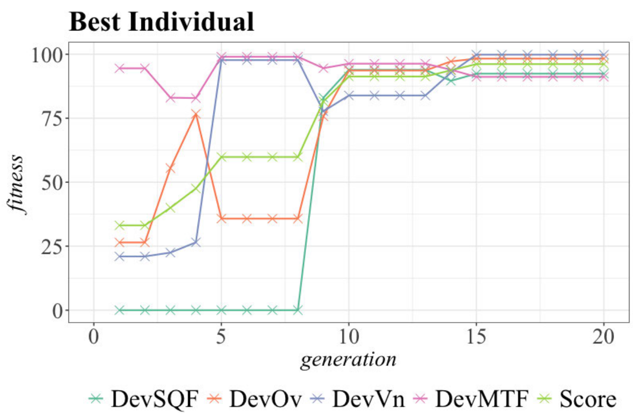

FIGURE 19. Evolution of the best individual of Test3.

verify that the evolution was alternating between yielding to being oversharpened by visual noise and vice versa until finding a balance of the two. This outcome may be because, in the objective function, both parameters are equally weighted. In turn, we see that MTF does not vary much over the generations, but we can see a certain relationship with visual noise since they tend to vary at the same time. In this test, it can be seen that, despite the fact that the objective values are not reached at 100%, in this case, the value of the visual noise and the oversharpening is quite high compared to the previous results.

In Table 7 and 8, the quality values achieved by the best individual and their ISP parameters are depicted.

TABLE 7. TEST3. Quality values obtained by the best individual of Test3.

IMAGE QUALITY ATTRIBUTES	VALUE
SQF	107.6
OvSha	3.71833333333
VNoise	25.0465
mtf50	0.318983333333

Comparing the values of the best individual with the default values (Table 2) and the values of Test3 (Table 8),

TABLE 8. TEST3. ISP parameters of the best individual of Test3.

ISP LIBRARY PARAMETERS	VALUE
Denoise Scale Y	[2.305172, 10.0, 5.183502, 7.496453]
Denoise Scale Chroma	[12.294407, 20.0, 5.382893, 1.533053]
Denoise Edge Softness Y	[5.577042, 12.980938, 15.0, 15.0]
Denoise Edge Softness Chroma	[10.970829, 5.913638, 1.0, 11.063793]
Denoise Weight Y	[0.045935, 0.039425, 0.0, 0.098158]
Lut	[0.236317, 5.910952, 3.836226, 0.0, 0.743372, 1.687434, 0.042223, 7.95, 5.328083, 3.19242, 5.31382, 1.268257, 5.626665, 7.95, 3.666799, 4.37531, 3.286383, 0.0, 7.04681, 0.0, 2.773487, 0.0, 7.95, 1.808277]

we can see that, in this case, the intensity of the noise reduction parameters is lower and somewhat less homogeneous. In Lut, we have that the function it describes remains quite abrupt, reaching many initial and final peaks. This result translates, as we will see again in photography, to a special type of edge sharpening with many artifacts and a very enlarged halo, which partly gives some diffuse sensations at various edges. On the other hand, it is verified that the introduction of a new image quality attribute (MTF) does not affect the optimization process. In Fig. 20, which corresponds to the photograph taken with this library, it can be seen that it gives a high sharpness sensation.

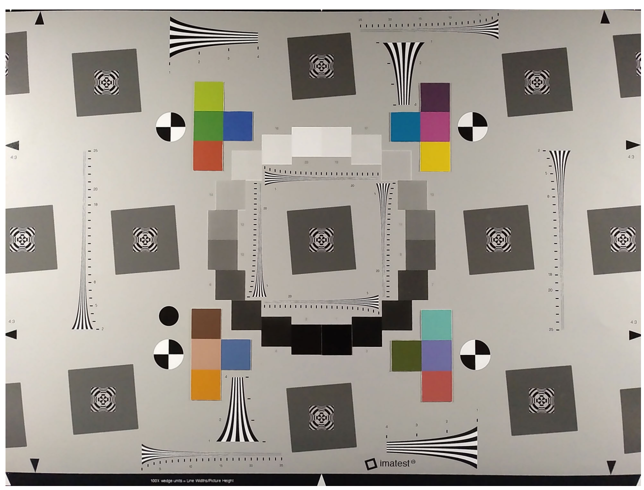

FIGURE 20. Photograph of the best individual of Test2.

This test has required 630 photographs, which took an approximate total time of 8 hours. This result implies that in 8 hours, a similar result has been achieved compared with those of previous tests; however, the number of generations required is significantly less than those of previous tests, indicating that we have found a better distribution of weights and evaluation criteria.

VI. CONCLUSION

In this article, the authors present a solution to the problem of the ISP tuning process. This process is usually performed manually by the camera tuning engineer through a trial and error process until finding the parameters that satisfy the image quality conditions. It is a very important and very complex process due to the large number of variables to take into account, which is why it is the best reason to use optimization algorithms to solve it. One of most substantial problems in this case is the quality criteria since photography has a great subjective factor. Not everyone likes the same intensity of color or definition of edges; however, there are certain quality standards that can be followed and formulas that allow us to evaluate many of them.

As a solution to this problem, we present a differential evolution algorithm that allows obtaining a first approximation of the ISP parameters. This evolutionary paradigm has been selected because it needs very few adjustment parameters and can find an acceptable solution with a small number of iterations due to its good exploration capacity [30]. Once the exploration task has been carried out, it will be the experts who will carry out the exploitation manually. The camera tuning engineer can easily perform fine-tuning to determine the final configuration, guided by his or her experience.

This article has addressed the challenge of adjusting many more ISP parameters than has ever been accomplished in previous work, as described in the introduction. Furthermore, as indicated in the state-of-the-art literature, this challenge remains an open problem in the engineering field. The described work shows that optimal ISP tuning allows for performance improvements in computer vision algorithms [15] and adaptability to different image acquisition conditions [16]. In [15], the authors propose automatic ISP tuning as a challenge for the future.

Future work includes improving the process in a way that reduces the time spent on each generation. The execution time of a generation is approximately 10-20 minutes. In future work, we envision parallelizing the implementation, which would considerably reduce the time of the generations. Another option, proposed by one reviewer, would be to simulate the software in such a way that we would avoid the time dedicated to the configuration/boot/shooting of the image. The idea would be to take an image, store it in raw mode and apply the differential evolution method with the simulator. In this sense, we would need to have an ISP software simulator that, at present, does not exist.

At the beginning of the project, it was thought to model the problem as a multi-objective problem. However, due to practicality issues, the expert engineers of Bq company wanted to have a control of the weight of each target to find a candidate region. From this region, they would perform the fine tuning. Anyway, the multi-objective version of the problem will be considered for an extension of the project.

As has been proven in the work, the optimization process has a high computing cost because it is necessary to modify, compile and load the library with the parameters of each individual. A possible improvement of the optimization process would be the application of surrogate models [31]. We can say that, during the optimization process, the only information we have about the objective function comes from the evaluation of each individual. Once the individual is evaluated, certain information is lost. A surrogate model aims to establish a correspondence between individuals and their evaluation in order to establish a meta-model that learns this correspondence. Once this correspondence is modelled, it could be used to estimate the evaluation of new individuals. The application of surrogate models can be a good approximation for future work related to ISP tuning, as it would probably accelerate the process.

REFERENCES

[1] H. S. Hawley and E. Robert McClain, "Visualizing sound directivity via smartphone sensors," *Phys. Teacher*, vol. 56, no. 2, pp. 72–74, 2018.

[2] N. Chandra, R. S. Chin, E. Cardova, M. D. Pratiwi, and Nadia, "Implementation of gyroscope sensor to presentation application on Android smartphone," in *Proc. Indonesian Assoc. for Pattern Recognit. Int. Conf. (INAPR)*, Sep. 2018, pp. 197–201.

[3] L. Wang, T. Gu, A. X. Liu, H. Yao, X. Tao, and J. Lu, "Assessing user mental workload for smartphone applications with built-in sensors," *IEEE Pervas. Comput.*, vol. 18, no. 1, pp. 59–70, Jan. 2019.

[4] M. M. Hassan, M. Z. Uddin, A. Mohamed, and A. Almogren, "A robust human activity recognition system using smartphone sensors and deep learning," *Future Gener. Comput. Syst.*, vol. 81, pp. 307–313, Apr. 2018.

[5] Y. Chen and C. Shen, "Performance analysis of smartphone-sensor behavior for human activity recognition," *IEEE Access*, vol. 5, pp. 3095–3110, 2017.

[6] T. Leeuw and E. Boss, "The HydroColor app: Above water measurements of remote sensing reflectance and turbidity using a smartphone camera," *Sensors*, vol. 18, no. 1, p. 256, Jan. 2018.

[7] R. Shea, D. Fu, A. Sun, C. Cai, X. Ma, X. Fan, W. Gong, and A. Liu, "Location-based augmented reality with pervasive smartphone sensors: Inside and beyond pokemon go," *IEEE Access*, 2017.

[8] B. P. Yan, C. K. Chan, C. K. Li, O. T. To, W. H. Lai, G. Tse, Y. C. Poh, and M.-Z. Poh, "Resting and postexercise heart rate detection from fingertip and facial photoplethysmography using a smartphone camera: A validation study," *JMIR mHealth uHealth*, vol. 5, no. 3, p. e33, Mar. 2017.

[9] M. S. Hossain and G. Muhammad, "An emotion recognition system for mobile applications," *IEEE Access*, vol. 7, pp. 2281–2287, 2017.

[10] W. Hauser, B. Neveu, J. B. Jourdain, C. Viard, and A. Guichard, "Image quality benchmark of computational Bokeh," *Electron. Imag.*, vol. 18, no. 21, pp. 340–341, 2018.

[11] A. Ignatov, R. Timofte, W. Chou, K. Wang, M. Wu, T. Hartley, and A. V. Gool, "AI benchmark: Running deep neural networks on Android smartphones," in *Proc. Eur. Conf. Comput. Vis.*, 2019, pp. 1–4.

[12] L.-L. Chen, R.-P. Han, and Y.-X. Bao, "Brief analysis of image signal processing for smart phone," in *Proc. Int. Conf. Comput., Mechatronics Electron. Eng.*, 2016, pp. 1–7.

[13] J. Nishimura, T. Gerasimow, R. Sushma, A. Sutic, C.-T. Wu, and G. Michael, "Automatic ISP image quality tuning using nonlinear optimization," in *Proc. 25th IEEE Int. Conf. Image Process. (ICIP)*, Oct. 2018, pp. 2471–2475.

[14] J. A. Nelder and R. Mead, "A simplex method for function minimization," *Comput. J.*, vol. 7, no. 4, pp. 308–313, Jan. 1965.

[15] L. Yahiaoui, J. Horgan, B. Deegan, S. Yogamani, C. Hughes, and P. Denny, "Overview and empirical analysis of ISP parameter tuning for visual perception in autonomous driving," *J. Imag.* vol. 5, no. 10, p. 78, 2019.

[16] M. Mody, S. Dabral, M. Magla, H. Sanghvi, N. Nandan, K. Chitnis, B. Jadhav, R. S. Allu, and G. Hua, "High quality image processing system for ADAS," in *Proc. IEEE Int. Conf. Electron., Comput. Commun. Technol. (CONECCT)*, Jul. 2019, pp. 1–4.
[17] M. Crepinsek, S. H. Liu, and M. Mernik, "Exploration and exploitation in evolutionary algorithms: A survey," *ACM Comput. Surv.*, vol. 45, no. 3, pp. 1–33, 2013.
[18] G. Olague, "Evolutionary computer vision: The 1st footprints," in *Natural Computing Series*. Berlin, Germany: Springer, 2016.
[19] R. Storn and K. Price, "Differential evolution—A simple and efficient adaptive scheme for global optimization over continuous spaces," *J. Global Optim.*, vol. 11, no. 4, pp. 341–359, 1995.
[20] R. Storn and K. Price, "Differential Evolution - A Simple and Efficient Heuristic for Global Optimization over Continuous Spaces," *J. Global Optim.*, 1997.
[21] S. Das, S. S. Mullick, and P. N. Suganthan, "Recent advances in differential evolution – an updated survey," *Swarm Evol. Comput.*, vol. 27, pp. 1–30, Apr. 2016.
[22] F. Neri and V. Tirronen, "Recent advances in differential evolution: A survey and experimental analysis," *Artif. Intell. Rev.*, vol. 33, nos. 1–2, pp. 61–106, Feb. 2010.
[23] S. Das, A. Abraham, U. K. Chakraborty, and A. Konar, "Differential evolution using a neighborhood-based mutation operator," *IEEE Trans. Evol. Comput.*, vol. 13, no. 3, pp. 526–553, Jun. 2009.
[24] *Automated Image Quality Analysis*, Imatest, Boulder, CO, USA, 2020.
[25] *IEEE Standard for Camera Phone Image Quality*, Standard 1858-2016, 2017.
[26] D. Glenn Boreman, "Modulation transfer function in optical and electro-optical systems," Tech. Rep., 2010. [Online]. Available: https://doi.org/10.1117/3.419857
[27] E. M. Granger and K. N. Cupery, "An optical merit function (SQF), which correlates with subjective image judgments," *Photograph. Sci. Eng.*, vol. 16, pp. 221–230, 1972.
[28] J. Brownlee, "Clever algorithms: Nature-inspired programming recipes," Tech. Rep., 2011. [Online]. Available: https://www.amazon.es/dp/1446785068?tag=amz-mkt-chr-es-21&ascsubtag=1ba00-01000-org00-mac00-other-nomod-es000-pcomp-feature-scomp-wm-5&ref=aa_scomp_sosp1
[29] D. H. Ackley, *A Connectionist Mach. for Genetic Hillclimbing*. Dordrecht, The Netherlands: Kluwer, 1987.
[30] A. W. Mohamed, "Differential evolution (DE): A short review," *Robot. Autom. Eng. J.*, vol. 2, no. 1, pp. 18–24, Jan. 2017.
[31] A. Diaz-Manriquez, G. Toscano-Pulido, and W. Gomez-Flores, "On the selection of surrogate models in evolutionary optimization algorithms," in *Proc. IEEE Congr. Evol. Comput. (CEC)*, Jun. 2011, pp. 2155–2162.

LUIS V. HEVIA received the degree in computer science from Carlos III University, in 2018. He is currently a DevOps Engineer with the MasMovil Group, Business Intelligence Department. His research interests include the applications of artificial intelligence in automation and optimization of processes.

MIGUEL A. PATRICIO (Member, IEEE) received the B.Sc. and M.Sc. degrees in computer science and the Ph.D. degree in artificial intelligence from the Universidad Politécnica de Madrid, in 1991, 1995, and 2002, respectively. He is currently an Associate Professor with the Escuela Politécnica Superior, Universidad Carlos III de Madrid. He is a coauthor of over 100 books, book chapters, journal articles, and technical reports; published by organizations, including Elsevier, IEEE, ACM, AAAI, Springer Verlag, and Kluwer; and most of these present practical and theoretical achievements of data analysis, computer vision, and distributed systems.

JOSÉ M. MOLINA (Member, IEEE) received the Ph.D. degree in telecommunications engineering from the Universidad Politécnica de Madrid. He is currently a Full Professor of computer science with the Carlos III University of Madrid. He also coordinates the Applied Artificial Intelligence Group. His research interests include applying soft-computing techniques to radar data processing, air traffic management, e-commerce, and ambient intelligence.

ANTONIO BERLANGA (Member, IEEE) received the degree in physics from the Autonomous University of Madrid, Spain, in 1995, and the Ph.D. degree in computer engineering from the Carlos III University of Madrid, in 2000. He has been an Associate Professor with the Computer Science Department, Universidad Carlos III de Madrid, since 2000. His research interests include evolutionary computation, multiobjective evolutionary algorithms, machine learning, and data mining.